J Mater Sci: Mater Electron (2017) 28:4951–4957
DOI 10.1007/s10854-016-6147-0

CrossMark

Frequency dependent C–V and G/ω–V characteristics on the illumination-induced Au/ZnO/n-GaAs Schottky barrier diodes

S. O. Tan[1] · H. Uslu Tecimer[2] · O. Çiçek[3] · H. Tecimer[4] · Ş. Altındal[5]

Received: 25 October 2016 / Accepted: 25 November 2016 / Published online: 29 November 2016
© Springer Science+Business Media New York 2016

Abstract Au/ZnO/n-GaAs Schottky barrier diodes (SBDs) have been examined by the capacitance–voltage (C–V) and conductance–voltage (G/ω–V) measurements. The frequency dependence characteristics of measurements were obtained under various illumination levels at room temperature. The C and G/ω relation was observed as the decrement in capacitance corresponds to an increment in conductance. The increment of negative capacitance (NC) values by high frequency at forward biases was ascribed to the series resistance, interface states and interfacial layer. Considering the illumination intensity, the NC values were observed to increase with the decreasing illumination while the G/ω values increase with the increasing illumination. This behavior was referred to the increments in the polarization and carriers in the SBDs. The adverse impacts of the voltage dependent resistivity were decreased with increasing illumination levels. Eventually, a strong interaction between the electrical properties of SBDs and the frequency, illumination and applied bias voltage was demonstrated by experimental results.

✉ S. O. Tan
serhatorkuntan@karabuk.edu.tr

H. Uslu Tecimer
habibeuslu@karabuk.edu.tr

O. Çiçek
ocicek@kastamonu.edu.tr

H. Tecimer
huseyintecimer@karabuk.edu.tr

Ş. Altındal
altundal@gazi.edu.tr

[1] Karabuk Vocational School, Karabuk University, Karabük, Turkey

[2] Department of Electrical and Electronic Engineering, Faculty of Engineering, Karabük University, Karabük, Turkey

[3] Arac Vocational School, Kastamonu University, Kastamonu, Turkey

[4] Department of Mechatronics Engineering, Faculty of Technology, Karabük University, Karabük, Turkey

[5] Department of Physics, Faculty of Science, Gazi University, Ankara, Turkey

1 Introduction

The number of scientific studies on a versatile semiconductor gallium arsenide (GaAs) has substantially increased in recent years with developing technology [1–4]. The evidence of being a multipurpose semiconductor is the usage of GaAs in wide variety of applications such as solar cells, field effect transistor (FET) devices, light emitting diodes (LEDs), microwave devices and other integrated circuit elements. High-speed and low-power devices exploit GaAs semiconductor for its direct forbidden bandgap, high electron mobility, lower power dissipation, high break-down voltage and mechanical stability properties [5–7]. Now, the evolvements on GaAs electronic devices provide extensive information about the characteristics of metal contacts on gallium arsenide semiconductor [8]. The performance of GaAs based metal–semiconductor (MS) devices is related with the parameters such as frequency, temperature, series resistance (R_s), applied bias voltage and interface defect density (N_{ss}) [7–11].

As it is well known, when a thin interfacial insulator is generated between interfaces of metal semiconductor (MS) contact, alias Schottky barrier diode (SBD), the structure is converted into metal-insulator-semiconductor (MIS) contact [12, 13]. The performance and also the reliability of the MIS SBD are acutely influenced by the quality of this

interface layer between deposited material and the semiconductor surface [14, 15]. Thus far a large variety of materials were used as an interface layer. Zinc oxide (ZnO), frequently utilized material in SBDs as a semiconductor, was distinctly used as an inorganic interfacial layer with GaAs based SBDs in this study. Laser diodes and room temperature polariton lasers, UV photodetectors, piezotronics, high power LEDs and many other applications are utilized with the wide bandgap ZnO by considering its superior properties such as high transparency, piezoelectricity, room-temperature ferromagnetism, etc [16–19].

Considering the ideal behavior, the dependency on the applied bias voltage increment causes an enhancement at the MIS type SBD capacitance [20, 21]. Although MIS structures are mostly independent from frequency at its high levels, the situation usually changes in the regions of depletion and accumulation at intermediate and lower frequencies by the effects of N_{ss}, R_s, surface charge and interface layer between M/S [22–24]. Generally, the AC signal tracking capability of the N_{ss} charges at low frequencies and the frequency dependent capacitance and conductance values of interface layer are the reason to this situation [23–26]. ZnO substantially changed the capacitance–voltage (C–V) and the conductance–voltage (G/ω–V) characteristics of the SBD as an interface layer in this study. The interface states densities and especially the series resistance on the C–V and G/ω–V characteristics lead to deviations from the ideal diode behavior. This also makes the measured values of C and G/ ω necessarily depend on frequency. Examining the frequency dispersion of C and G/ω, it is so important to handle the effect of the R_s and N_{ss} firmly [27]. Herewith, other crucial factors such as metal to semiconductor barrier height (Φ_b) and thickness of interfacial insulator layer (d_{ox}) can also bring the structure to the non-ideal case [22]. Having remarkable optical properties, the presence of ZnO caused to investigate the illumination intensity dependency of the variations on the values of capacitance and conductance under forward and reverse biases almost at low and high frequencies. The electrical parameters of SBDs are exceptionally relevant with the intensity of illumination level, so the analysis of SBDs should be made not only in dark but also in different illumination levels to inform the structural parameters of devices [28].

Recently, negative capacitance (NC) behavior has been realized by some researchers as an ill-defined peak and its concept has not been exactly comprehended yet [29–34]. The general consensus on NC in the forward bias/accumulation region is the existence of surface states (N_{ss}) and their relaxation time (τ), series resistance (R_s), the contact injection and minority carrier injection [29–31]. The loss of interface charge at occupied states below Fermi energy level (E_F) due to impact ionization is the other reason of NC [32]. On the other hand, sometimes, NC behavior can be attributed to instrumental problems, such as parasitic inductance or poor measurement equipment calibration, respectively [29, 32]. We think that the observations of NC by researchers were not reported in the literature to prevent any confusion. Therefore, in general, the NC has been referred to as "anomalous" or "abnormal" behavior in the literature [29–33]. The NC behavior phenomenon can be explained as the material exposes an inductive behavior. Hitherto, the studies carried out in NC behavior have shown that this behavior can be observed in forward bias region at different frequencies and temperatures [29, 34]. Based on a study, the injection of minority carriers brings out the NC behavior that can only be observed at forward bias and low frequencies [35]. The physical mechanism of the NC acts on distinct devices is evidently different. Although the injection of charge carriers involves a hopping process to localized interface traps/states, the physical mechanism of the injection has not diffusively understood yet [30]. NC can be expressed practically with the behavior of the temperature and frequency dependent admittance spectroscopy (C–V and G/ω–V) data [36].

The Au/ZnO/n-GaAs SBDs I–V characteristics at both biases were investigated in darkness and also distinct illumination levels in our previous study [5]. As a continuation of that study, the frequency dependence of C–V and G/ω–V characteristics of the Au/ZnO/n-GaAs SBDs were investigated in illumination range of 0–200 W at room temperature in this study. The effects of R_s, N_{ss} and interfacial layer were investigated at SBD from the C–V measurements which are also recruiting to find out the source of NC. The voltage dependence of the resistivity R_i was also obtained from measurements of C–V and G/ω–V plots for a given bias voltage for each illumination levels.

2 Experimental procedure

The wafer n-type GaAs (100) with 300 µm thickness and 1–10 Ω cm resistivity was used as substrate to prepare Au/ZnO/n-GaAs/Au device. GaAs was cut into pieces of 1.0 cm length by 1.0 cm breadth and chemically cleaned using acetone, isopropyl alcohol ultrasonic cleaner for 5 min. After cleaning process, it quenched in de-ionized water. The ohmic contact was formed on the backside of the n-GaAs substrate by the evaporation of the 150 nm gold (Au) in high purity (99.999%). After annealing the contact in N_2 atmosphere for 3 min at 400 °C, the native oxide on the leading surface of substrate was removed by applying $HF + 10H_2O$ solution. Before drying the contact with N_2, 30 s rinse process was applied in de-ionized water. RF sputter technique was used to grow ZnO (50 nm) film on n-GaAs substrates and the thickness was also controlled by the thickness monitor. The construction of the Schottky

diodes with an area of 7.85×10^{-3} cm^2 was finalized by thermal evaporating Au (150 nm) as dots with 1.0 mm diameter on the forepart of the ZnO/n-GaAs/Au. The vacuum coating unit at 4.10^{-6} Torr was used for the processes of evaporation and coating.

Hewlett Packard 4192A LF Impedance Analyzer (5 Hz–13 MHz) was used to implement the C–V measurements of the diode. As a light source 250 W solar simulator Newport-Oriel with a model number of 69931 was applied to illuminate the sample. The illumination intensity was measured by a research radiometer of International Light Technologies ILT1700. The Janis vpf-475 cryostat contributed to the measurements by decreasing the noise. AC/DC converter card IEEE-488 in cryostat was also used to perform the measurements. Figure 1 presents the symbolic diagram of the Au/ZnO/n-GaAs SBD structure under light source.

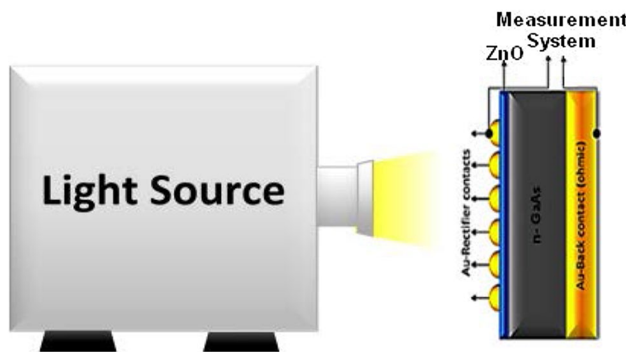

Fig. 1 The connection of the measurement system to Au/ZnO/n-GaAs SBDs under a light source

3 Results and discussion

The Au/ZnO/n-GaAs Schottky barrier diodes (SBDs) characteristics of capacitance (C) and conductance (G/ω) versus voltage (V) were examined in the illumination range of 0–200 W at room temperature. These characteristics at 10 and 500 kHz were displayed in Figs. 2 and 3 respectively. The MIS type SBDs behavior was observed from the inversion, depletion and accumulation regions which are plainly shown in figures for each illumination. The variation of C and G/ω values are from the strong inversion region (−5 V) to the strong accumulation region (4 V).

The capacitance values in Fig. 2a increased with increasing applied bias voltage up to accumulation region at 4 V. The reason of the distinctive curvature in this accumulation region generally can be interpreted as the effect of R_s. When the capacitance values handled in terms of frequency from Fig. 2, an increment in frequency from 10 to 500 kHz caused a decrement in capacitance values. The existence of the interface states is the main reason of the frequency dependence of the capacitance [37]. As mentioned above, AC signal tracking of N_{ss} is easier at low frequencies, and this situation reflects as an enhancement on the capacitance of the measurement values. Contrary to this, AC signal cannot be followed by the interface states at high frequencies, and the interface variance do not promote the capacitance anymore [37, 38]. So, the more specific peak seen in the C–V plot at 10 kHz can be related to the particular density distribution of N_{ss}. On the contrary, the capacitance peak value began to decline and turned towards the negative biases and the negative capacitance (NC) observed by the frequency increment to the 500 kHz in Fig. 2b. It is clearly seen in Fig. 2a that the NC values disappear at 10 kHz frequency.

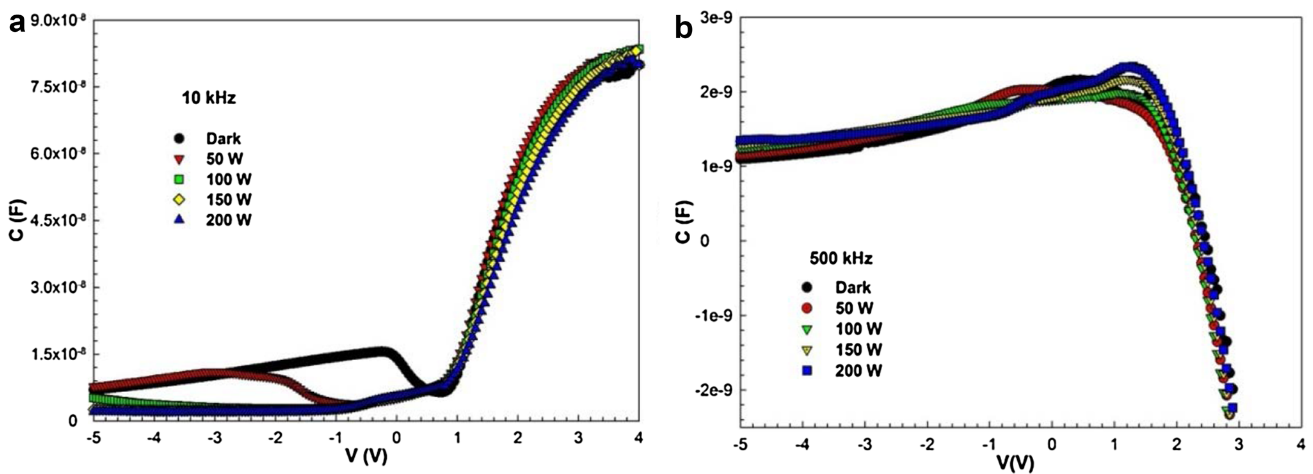

Fig. 2 The experimental C–V characteristics of Au/ZnO/n-GaAs SBD at **a** 10 kHz, **b** 500 kHz

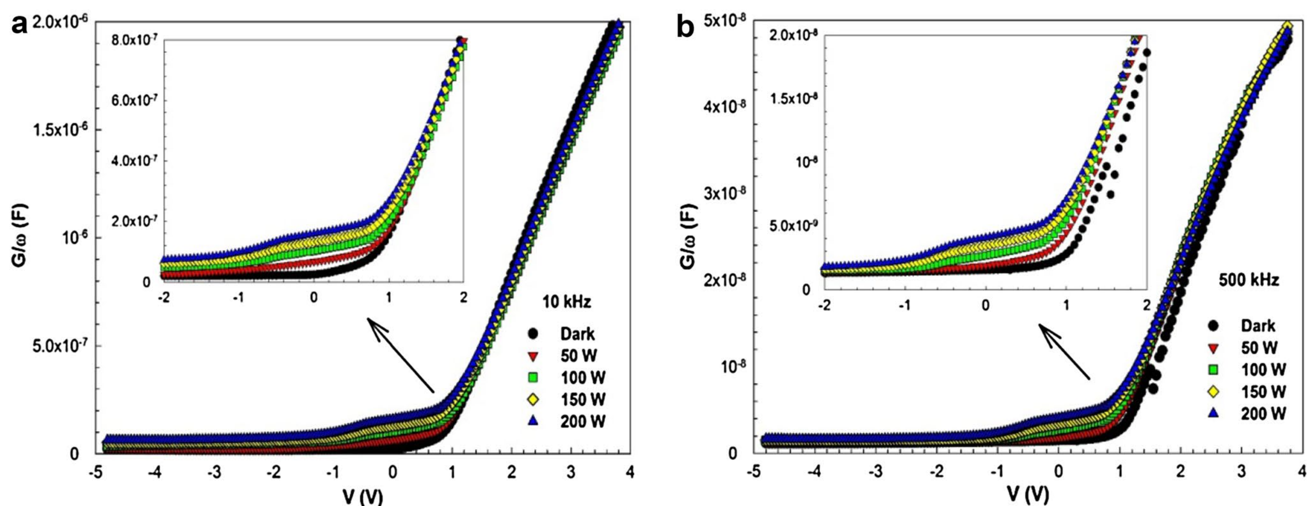

Fig. 3 The experimental G/ω–V characteristics of Au/ZnO/n-GaAs SBD at **a** 10 kHz **b** 500 kHz

The conductance–voltage (G/ω–V) measurements imply the voltage effect at two specific frequencies on the SBDs conductance as shown in Fig. 3. As displayed in Fig. 3a, b, the conductance of the Au/ZnO/n-GaAs SBDs depends on frequency as well as on voltage. It is observed that the increment in the frequency leads to the decrement in the conductance of the diode.

The C–V and G/ω–V curves were also drawn for adequately high frequency (500 kHz) and low frequency (10 kHz) to compare the inductive behavior. It is obviously extracted from Figs. 2 and 3 that the variation of the frequency and the applied bias voltage on the measured C and G/ω values are represented impressively in the depletion and accumulation regions rather than the inversion region and the decrease in the capacitance corresponds to an increase in conductance.

The negative value of C increases at high frequency (500 kHz) and such behavior of C in the forward bias was credited to the loss of charges located at surface interface states/traps, series resistance, thickness of interfacial layer and doping concentration as similarly reported several times in the literature [25, 26, 29, 37–40].

The effectuality of illumination intensity on conductance and capacitance properties in dark and 100 W at 500 kHz are presented in Fig. 4. It is observed that the values of C and G/ω increases quietly with illumination enhancement to 100 W in the entire bias at this high frequency of 500 kHz. The illumination effectuality on Au/polyvinyl alcohol (Co, Zn doped)/n-Si SBD have also been studied by Uslu et al. resulting as an increment at the device capacitance with increase in illumination intensity [41].

The comparison of the C and G/ω variation at the same bias voltage range, the C–V and G/ω–V plots of Au/ZnO/n-GaAs SBDs for 500 kHz in dark and 100 W are given in Fig. 4a, b. After C–V reaches the peak value, the decrement in the capacitance values with the increasing bias voltage

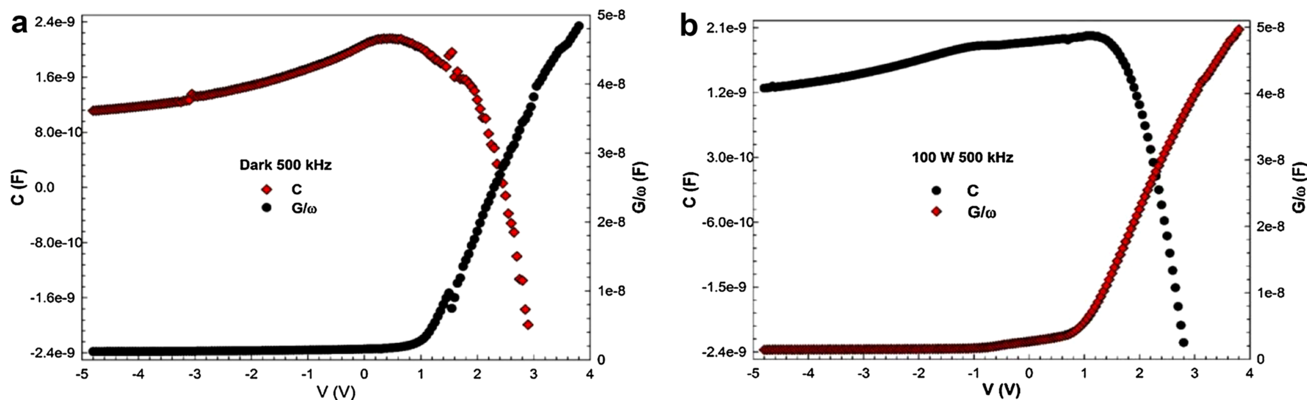

Fig. 4 The variation of the C–V and G/ω–V for the Au/ZnO/n-GaAs SBD **a** in dark **b** at 100 W

can be seen in Fig. 4. The C values decrease and converge to the negative values at about 2.5 V. Conversely, the values of G/ω increase in direct proportion to the bias voltage in the entire bias region. Apparently, the decrement in the C corresponds to an increment in the G/w and this behavior of C and G/ω points out that the material displays an inductive behavior [32, 33]. However, the minimum capacitance values coincide with the maximum conductance values at 3 V of forward biases. It is considered as the polarization increment decreases the C value and more carriers are acquainted in the structure. As affirmed by the C–V measurements, the negative capacitance impact upon the SBD was formed by the R_s, interface states and N_{ss} at forward biases related with the applied forward bias voltage shared between the semiconductor and interfacial layer. The loss of interface charges leads to the NC behavior and this can be interpreted by the charge injection, minority-carrier injection or N_{ss} effects in several electronic devices [32, 33]. Thus, the characteristics of C–V and G/ω–V implied that negative capacitance existence appeared at specific high frequency of 500 kHz under both darkness and 100 W illumination corresponds to the maximum conductance of the SBD.

Considering the ideal C and G/ω versus voltage characteristics behavior, series resistance parameter, as denoted by R_s, has a significant effect on SBD. The plots in Fig. 5 present voltage dependence of the resistivity R_i which were extracted from measurements of C–V and G/ω–V for a given bias voltage for each illumination levels. The values of resistivity R_i were extracted by Nicollian and Brews method in all three regions known as inversion/reverse, depletion and accumulation respectively. The real value of R_s can also be obtained from this method in the strong accumulation region [42].

Rs can also cause a serious error in the extraction of electrical and dielectric properties. The value of R_s is effective especially at the accumulation region and it can originate from various sources such as the back ohmic contact to the semiconductor, the contact made by the probe wire to the gate or rectifier contact, the resistance of bulk of the semiconductor, a dirt film or particulate matter at back contact/pedestal interface and extremely non-uniform doped atoms in the semiconductor [1, 13]. The magnitude of R_s can be reduced either by having a low BH at M/S interface or by having an enhanced tunneling through the barrier by using heavy doped semiconductors ($\geq 10^{17}$ cm^{-3}) or by the use of a good cleaning and fabrication process. The resistance at high forward biases corresponds to the real value of R_s while the resistance at high reverse bias corresponds to the R_{sh} for the diode. The lower R_s and the higher R_{sh} requirements for the ideal diode were obtained here and as seen in Fig. 5. the R_{sh} values decrease at the reverse biases while the R_s values are almost not changed with increasing illumination levels [37].

Consequently, as a general opinion, Nicollian and Brews method accurately determines voltage dependence resistivity of SBDs for both two biases regions. R_i values were given by using this method as:

$$R_i = \frac{G_m}{G_m^2 + \omega^2 C_m^2} \tag{1}$$

The measured capacitance and conductance values under darkness and various illumination levels for low and high frequencies at given voltage are denoted by C_m and G_m. The calculations of R_i values in Fig. 5a, b were obtained from the both data in Figs. 2 and 3.

The decrement of the calculated R_s values with increasing temperature is ascribed to the particular distribution of localized interface states [38]. Interface charge, oxide-trapped charge and other frequency-dependent charges are the main reason of this frequency dependence of R_s. The

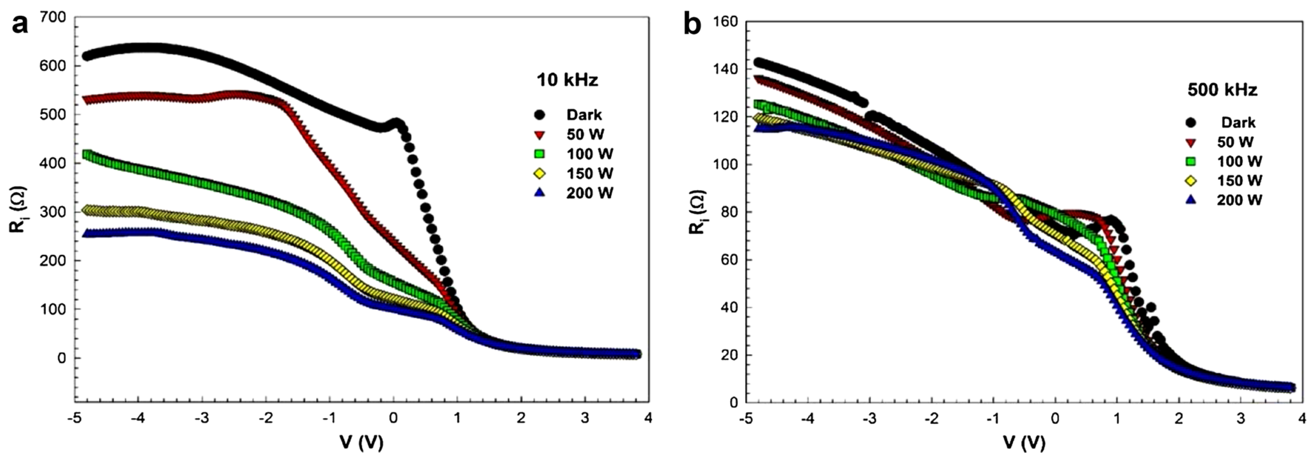

Fig. 5 The experimental R_i–V characteristics of Au/ZnO/n-GaAs SBD at **a** 10 kHz **b** 500 kHz

R_s in the device should be taken into account to achieve the C_m and G_m values [37].

These outstanding values request particular relevance to be uncovered the effects of the R_i on the C and G/ω versus voltage characteristics. Although the weak illumination dependency of R_i values on high bias voltages were observed in accumulation regions of Fig. 5, the evaluation for each bias voltage should be made as the increment of illumination intensity causes a decrement at R_i values. As also indicated in Fig. 5, the values of R_i decreases for each illumination levels with the increasing applied biases. The strong dependency of R_i values on illumination at reverse bias region emerges as a striking feature of Fig. 5.

As a result, the presence of this difference is due to the nature of measured applied bias voltage. When the sample is biased under the forward direction, the external electric and inner electric field is opposite to each other and so total electric field becomes decrease. In this case, the generation electron–hole pairs soon converge and neutralize and so cannot yield any excess current to the dark current. On the other hand, the situation is thoroughly different under rewire bias condition. In other words, under reverse condition, both external and inner electric field is same direction and so the total electric field becomes very strong in the respect of forward biases. Thus, the generation electron–hole pairs will easy separated each other's and yield an excess current to the dark current. Therefore, the photo current or photo conductivity under reverse bias always is greater than the forward biases.

4 Conclusion

The frequency dependence of C–V and G/w–V characteristics of the Au/ZnO/n-GaAs SBDs were investigated in illumination range of 0–200 W at room temperature. In the light of the experimental results, the strong dependency of the C–V and G/ω–V characteristics on applied biases and frequency were clearly outlined. The increment of the bias voltage provided an increment in capacitance values at 10 kHz. Contrarily, when the frequency increased to a high value of 500 kHz, the values of C decreased and started to take negative values for the forward bias voltages at about 2.5 V. The increment in the frequency led to the decrement in the conductance of the Au/ZnO/n-GaAs SBD and this can be explained by the effect of high frequencies on the conductance of the diode. The relation between C and G/ω was emerged as the decrease in the capacitance corresponds to an increase in conductance. The enhancement of the NC values at 500 kHz was related to the interface states, series resistance, loss of charges located at surface of the interfacial layer. The illumination effect was also utilized from the measurements and the negatively obtained C values increase with the decreasing illumination while the G/ω values increase with the increasing illumination at the forward bias voltage. Such behavior of the capacitance and conductance can be attributed to the increments in the polarization and carriers in the SBD structure. The admittance measurements were obtained from Nicollian and Brews methods to uncover the voltage dependent profile of R_s. The effects of illumination increment were especially observed in the reverse bias region as a decrement on R_i values. Experimental results indicate that the under-researched electrical properties of the SBD are quite sensitive to frequency, illumination and applied bias voltage.

Acknowledgements This study has been funded by Scientific Research Project (BAP) Coordinatorship of Karabuk University with project codes of KBU-BAP-14/2-DR-005 & KBU-BAP-14/2-DR-006.

References

1. S.M. Sze, *Physics Semiconductor Devices*. (Wiley, New York, 1981)
2. P. Macháč, V. Peřina, J. Mater. Sci. Mater. Electron. **23**, 2282–2288 (2012)
3. D. Korucu, H. Efeoglu, A. Turut, Ş. Altındal, Mater. Sci. Semicond. Proc. **15**, 480–485 (2012). doi:10.1016/j.mssp.2012.03.005
4. T.S. Huang, R.S. Fang, Solid State Electron. **37**, 1461–1466 (1994). doi:10.1016/0038-1101(94)90152
5. S.O. Tan, H. Uslu Tecimer, O. Çiçek, H. Tecimer, İ. Orak, Ş. Altındal, J. Mater. Sci. Mater. Electron. **27**, 8340–8347 (2016). doi:10.1007/s10854-016-4843-4
6. M. E. Aydın, M. Soylu, F. Yakuphanoglu, W.A. Farooq, Microelectron. Eng. **88**, 867–871 (2011). doi:10.1016/j.mee.2010.11.012
7. S. Demirezen, E. Özavcı, Ş. Altındal, Mater. Sci. Semicond. Proc. **23**, 1–6 (2014). doi:10.1016/j.mssp.2014.02.022
8. J.M. Borrego, R.J. Gutmann, S. Ashok, Solid State Electron. **20**, 125–132 (1977)
9. F.A. Padovani, G.G. Sumner, J. Appl. Phys **36**, 3744–3747 (1965)
10. A.T. Sharma, Shahnawaz, S. Kumar, Y.S. Katharria, D. Kanjilal, Nucl. Instr. Meth. Phys. Res. B **263**, 424 (2007)
11. M.K. Hudait, P. Venkateswarlu, S.B. Krupanidhi, Solid State Electron. **45**, 133–141 (2001)
12. N. Başman, O. Uzun, S. Fiat, C. Alkan, G. Çankaya, J. Mater. Sci. Mater. Electron. **13**, 273–275 (2002). doi:10.1007/s10854-012-0819-1
13. S. Demirezen, Ş. Altındal, İ. Uslu, Current, Appl. Phys **13**, 53–59 (2013)
14. T.T.A. Tuan, D.-H. Kuo, C.-C. Li, W.-C. Yen, J. Mater. Sci. Mater. Electron. **25**, 3264–3270 (2014). doi:10.1007/s10854-014-2012-1
15. V.V. lchenko, V.V. Marin, S.D. Lin, K.Y. Panarn, A.A. Buyanin, O.V. Tretyak, J. Phys. D Appl. Phys. **41**, 235107 (2008)
16. J.K. Jha, R. S.-Ortiz, J. Du, N.D. Shepherd, J. Mater. Sci. Mater. Electron. **25**, 1492–1498 (2014). doi:10.1007/s10854-014-1758-9
17. D. Ahn, S.-H. Park, Measurement **46**, 1698–1703 (2013). doi:10.1016/j.measurement.2013.01.004
18. C. Tsiarapas, D. Girginoudi, N. Georgoulas, Superlattices Microstruct. **75**, 171–182 (2014). doi:10.1016/j.spmi.2014.07.041

19. C.S. Singh, G. Agarwal, G. Durga Rao, Sujeet Chaudhary, R. Singh, Mater. Sci. Semicond. Proc. **14**, 1–4 (2011). doi:10.1016/j.mssp.2010.12.009
20. E.H. Rhoderick, R.H. Williams, *Metal–Semiconductor Contacts*, (Clarandon Press, Oxford University Press, Cambridge, 1988), pp. 20–45
21. A. Singh, Solid State Electron. **28**, 223–232 (1985)
22. H.C. Card, E.H. Rhoderick, J Phys D **4**, 1589–1601 (1971)
23. V. R. Reddy, V. Janardhanam, M.-S. Kang, C.-J. Choi, J. Mater. Sci. Mater. Electron. **25**, 2379–2386 (2014). doi:10.1007/s10854-012-0819-1
24. J. Bisquert, G. Garcia-Belmonte, A. Pitarch, H.J. Bolink, Chem. Phys. Lett. **422**, 184–191 (2006)
25. P. Chattopadhyay, B. Raychaudhuri, Solid State Electron. **35**, 875–892 (1992)
26. P. Cova, A. Sing, R.A. Masut, J. Appl. Phys **82**, 5217–5226 (1997)
27. S. Zeyrek, E. Acaroğlu, Ş. Altındal, S. Birdoğan, M.M. Bülbül, Curr. Appl. Phys. **13**, 1225–1230 (2013)
28. H. Uslu, Ş. Altındal, U. Aydemir, İ. Dökme, İ.M. Afandiyeva, J. Alloys Compd. **503**, 96–102 (2010)
29. E. Arslan, Y. Şafak, Ş. Altındal, Ö. Kelekçi, E. Özbay. J. Non-Cryst. Solids **356**, 1006–1011 (2010)
30. J. Werner, A.F.J. Levi, R.T. Tung, M. Anzlowar, M. Pinto, Phys. Rev. Lett. **60**, 53 (1988)
31. M. Ershov, H.C. Liu, L. Li, M. Buchanan, Z.R. Wasilewski, A.K. Jonscher, IEEE Trans. Electron Devices **45**, 2196 (1998)
32. A.A. Al-Ghamdi, A. Dere, A. Tataroğlu, B. Arif, F. Yakuphanoglu, F. El-Tantawy, W.A. Farooq, J. Alloy Compd. **650**, 692–699 (2015)
34. H.G. Çetinkaya, D.E. Yıldız, Ş. Altındal, Int. J. Mod. Phys. B. **29** 1450237 (2015). doi:10.1142/S0217979214502373
35. A.G.U. Perera, W.Z. Shen, M. Ershov, H.C. Liu, M. Buchanan, W.J. Schaff, App. Phys. Lett. **74**, 3167 (1999)
36. C.H. Champness, W.R. Clark, App. Phys. Lett. **56**(12), 1104–1106 (1990). doi:10.1063/1.102581
37. X. Wu, E.S. Yang, H.L. Evans, J. Appl. Phys. **68**, 2845 (1990). doi:10.1063/1.346442
38. A. Tataroğlu, O. Dayan, N. Özdemir, Z. Şerbetci, A.A. Al-Ghamdi, A. Dere, F. El-Tantawy, F. Yakuphanoglu, Dyes Pigments **132**, 64–71 (2016). doi:10.1016/j.dyepig.2016.04.044
39. A.S. Dahlan, A. Tataroğlu, A.A. Al-Ghamdi, A.A. Al-Ghamdi, S. Bin-Omran, Y. Al-Turki, F. El-Tantawy, F. Yakuphanoglu, J. Alloy Compd. **646**, 1151–1156 (2015)
40. H. Yan, E. Shunsuke, H. Yusuke, O. Hidenori, Chem. Lett. **36**(8), 986–990 (2007)
41. R.L. Van Meirhaeghe, W.H. Lafle´re, F. Cardon, J. Appl. Phys. **76** 403–406 (1994). doi:10.1063/1.357089
42. H. Uslu, S. Altındal, I. Dokme, J. Appl. Phys **108**, 104501 (2010)
43. E.H. Nicollian, J.R. Brews, *Metal Oxide Semiconductor (MOS) Physics and Technology*. (Wiley, New York, 1982)